Tomosyn-1 is involved in a post-docking event required for pancreatic β-cell exocytosis

Séverine Cheviet[1], Paola Bezzi[1], Rosita Ivarsson[2], Erik Renström[2], David Viertl[3], Sandor Kasas[1,3], Stefan Catsicas[3] and Romano Regazzi[1,*]

[1]Department of Cell Biology and Morphology, Rue du Bugnon 9, University of Lausanne, 1005 Lausanne, Switzerland
[2]Department of Clinical Sciences, Malmö, Lund University, Sweden
[3]Laboratoire de Neurobiologie Cellulaire, Ecole Polytechnique Fédérale, Lausanne, Switzerland
*Author for correspondence (e-mail: Romano.Regazzi@unil.ch)

Accepted 5 May 2006
Journal of Cell Science 119, 2912-2920 Published by The Company of Biologists 2006
doi:10.1242/jcs.03037

Summary

Although the assembly of a ternary complex between the SNARE proteins syntaxin-1, SNAP25 and VAMP2 is known to be crucial for insulin exocytosis, the mechanisms controlling this key event are poorly understood. We found that pancreatic β-cells express different isoforms of tomosyn-1, a syntaxin-1-binding protein possessing a SNARE-like motif. Using atomic force microscopy we show that the SNARE-like domain of tomosyn-1 can form a complex with syntaxin-1 and SNAP25 but displays binding forces that are weaker than those observed for VAMP2 (237±13 versus 279±3 pN). In pancreatic β-cells tomosyn-1 was found to be concentrated in cellular compartments enriched in insulin-containing secretory granules. Silencing of tomosyn-1 in the rat β-cell line INS-1E by RNA interference did not affect the number of secretory granules docked at the plasma membrane but led to a reduction in stimulus-induced exocytosis. Replacement of endogenous tomosyn-1 with mouse tomosyn-1, which differs in the nucleotide sequence from its rat homologue and escapes silencing, restored a normal secretory rate. Taken together, our data suggest that tomosyn-1 is involved in a post-docking event that prepares secretory granules for fusion and is necessary to sustain exocytosis of pancreatic β-cells in response to insulin secretagogues.

Key words: Insulin, Exocytosis, SNARE, TIRF

Introduction

Insulin secretion from pancreatic β-cells is an essential prerequisite to maintain appropriate blood glucose levels. Defects in this process can result in profound metabolic disorders and, eventually, lead to diabetes mellitus. The molecular mechanism regulating the fusion of insulin-containing secretory granules with the plasma membrane are beginning to be understood. Studies performed during the last few years have highlighted a central role for several components of the machinery of neurotransmitter release in the exocytotic process of pancreatic β-cells (Lang, 1999; Easom, 2000; Rorsman and Renström, 2003). These components include the SNAREs (soluble-*N*-ethylmaleimide-sensitive factor attachment protein receptor) VAMP2, SNAP25 and syntaxin-1. SNAREs constitute a large family of evolutionarily conserved proteins that are essential for intracellular vesicular transport and for exocytosis (Bock et al., 2001). The members of the SNARE family are characterized by the presence of one or more 60 amino acid α-helical domains referred to as SNARE-motifs. Depending upon the presence of arginine or glutamine residues in the core of their α-helical domains SNAREs are classified as R- or Q-SNAREs (Fasshauer et al., 1998). VAMP2 is an R-SNARE inserted in the membrane of insulin-containing secretory granules whereas SNAP25 and syntaxin-1 are Q-SNAREs located at the β-cell membrane. During the final events leading to exocytosis the R-SNARE motif of VAMP2, the two Q-SNARE motifs of SNAP25 and the Q-SNARE motif of syntaxin-1 arrange in parallel to form a thermodynamically highly favorable four-helix bundle. According to current models, the formation of this SNARE complex forces granule and plasma membranes in close apposition and promotes bilayer fusion (Mayer, 2001).

Whereas the central role for VAMP2, SNAP25 and syntaxin-1 in neurotransmitter release and insulin exocytosis is now well recognized, the mechanisms regulating the assembly of the SNARE complex are not well understood. A large number of accessory factors that interact with SNAREs and positively or negatively influence the assembly of the complex have been identified (Gerst, 2003). Tomosyn is a 130 kDa syntaxin-1-binding protein first isolated from rat brain extracts (Fujita et al., 1998) that belongs to this group of regulatory proteins. In mammalian brain, two distinct genes drive the expression of seven closely related isoforms (b-tomosyn-1, m-tomosyn-1, s-tomosyn-1, xb-tomosyn-2, b-tomosyn2, m-tomosyn-2 and s-tomosyn-2) with distinct distribution patterns (Yokoyama et al., 1999; Groffen et al., 2005). All tomosyn isoforms possess a large N-terminal domain that contain WD40 repeats of unknown function, and a small C-terminal domain including an R-SNARE-like motif (Masuda et al., 1998). The SNARE-like properties enables the interaction of tomosyn with syntaxin-1 and allows the replacement of VAMP2 in the assembly of a heterotrimeric complex with SNAP25 (Hatsuzawa et al., 2003). Because of these findings, the role of tomosyn in various SNARE-mediated fusion processes has been investigated. tomosyn-1 was demonstrated to play an important function in growth-cone extension. This SNARE-

interacting protein was found to prevent the fusion of plasmalemmal precursor vesicles at the palm of the growth cones, thus promoting transport to the leading edges of growth cones (Sakisaka et al., 2004). Tomosyn-1 was also shown to be involved in exocytosis. Thus, overexpression of tomosyn-1 was reported to inhibit secretion of dense core granules in PC12 and chromaffin cells and in neurons (Hatsuzawa et al., 2003; Yizhar et al., 2004; Baba et al., 2005). This effect was attributed to impairment in Ca^{2+}-dependent vesicle priming and to a consequent reduction in the number of readily releasable vesicles (Yizhar et al., 2004).

In this study, we demonstrate that pancreatic β-cells express different tomosyn-1 isoforms and that silencing of the gene by RNA interference results in a decrease in stimulated exocytosis. Kinetics and imaging analysis revealed that the defect in exocytosis observed in the absence of tomosyn-1 occurs in a late event in the secretory pathway after the docking of insulin-containing granules with the plasma membrane.

Results

Tomosyn-1 is expressed in pancreatic islets

The components of the neuronal SNARE complex syntaxin-1, SNAP25 and VAMP2 are central constituents of the exocytotic machinery of pancreatic β-cells (Lang, 1999; Easom, 2000; Rorsman and Renström, 2003). However, so far the expression of the syntaxin-1-binding protein tomosyn-1 in pancreatic islets was not investigated. Immunohistochemical analysis of rat pancreatic sections revealed that tomosyn-1 is readily detected in all pancreatic islet cells, including insulin-positive cells (Fig. 1). Lower levels of tomosyn-1 immunoreactivity were also observed in the exocrine pancreas (Fig. 1).

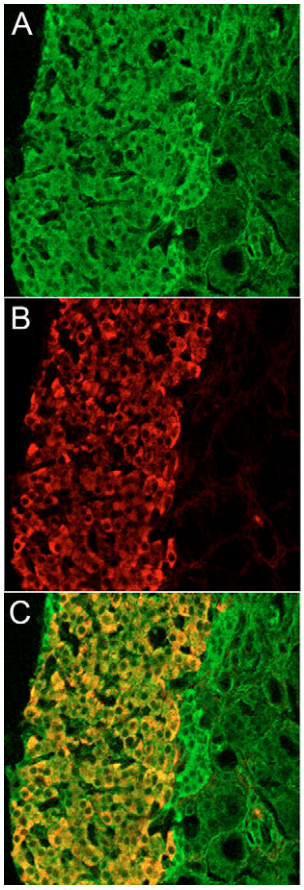

Fig. 1. Tomosyn-1 is expressed in rat pancreatic islets. Rat pancreatic sections were incubated with a polyclonal antibody directed against tomosyn-1 (Hatsuzawa et al., 2003) and a guinea pig antibody against insulin. (A) Expression of tomosyn-1 was assessed by confocal microscopy after labeling with an anti-rabbit antibody coupled to FITC. (B) Insulin-containing cells were visualized with an anti-guinea pig antibody coupled to Cy3. (C) Overlay.

Insulin-secreting cells express b-, m- and s-tomosyn-1

The gene encoding tomosyn-1 drives the expression of three splicing variants of the protein displaying different tissue distributions. b-tomosyn-1 is ubiquitously expressed, m-tomosyn-1 is mainly detected in brain and testis, and s-tomosyn-1 is restricted to brain (Yokoyama et al., 1999). To determine which isoform is expressed in β-cells, we performed reverse transcriptase (RT)-PCR analysis on mRNAs obtained from brain, pancreatic islets and from the two insulin-secreting cell lines, INS-1E and MIN6, using set of primers allowing selective amplification of each of the three isoforms. As expected, in brain extracts the three tomosyn-1 isoforms (b-, m- and s-tomosyn-1) were detected (Fig. 2). INS-1E cells displayed an expression pattern analogous to that of brain and similar levels of the three isoforms were amplified. In mRNA extracts of rat pancreatic islets and of MIN6 cells the predominant isoform amplified was m-tomosyn-1. Smaller levels of b-tomosyn-1 were also detected in these samples (Fig. 2).

Subcellular distribution of tomosyn-1

As an initial indication of the possible function of tomosyn-1 in β-cells, we determined the subcellular distribution of the protein. After ultracentrifugation of post-nuclear extracts of INS-1E cells, tomosyn-1 was recovered both in the supernatant and in the membrane pellet, indicating that at least part of the protein is associated with cellular organelles (data not shown). Analysis by confocal microscopy of INS-1E cells revealed that tomosyn-1 is not homogenously distributed throughout the cell. Indeed, a fraction of the protein was localized in cellular compartments enriched in secretory granules (Fig. 3). A similar distribution was observed in the mouse insulin-secreting cell line MIN6 (not shown). To further verify the association of tomosyn-1 with secretory vesicles, a post-nuclear supernatant of INS-1E cells was analyzed on a sucrose density gradient (Cheviet et al., 2004). As shown in Fig. 4, tomosyn-1 co-sedimented with the insulin-containing secretory granule marker granuphilin but not with synaptophysin, a marker of synaptic-like microvesicles. These finding confirms that at least a fraction of tomosyn-1 is associated with insulin granules.

Silencing of tomosyn-1 results in a decrease in insulin exocytosis

Next, we investigated the involvement of tomosyn-1 in insulin exocytosis by selectively reducing its expression level. For this purpose, we took advantage of the possibilities offered by the RNA interference process. We generated two plasmids that direct the synthesis of small interfering RNAs (siRNAs) targeted against the sequence of rat tomosyn-1. Transfection of siRNA-a into COS cells resulted in a very strong reduction in

the expression of both GFP-tagged rat tomosyn-1 and of the endogenously expressed monkey tomosyn-1 (Fig. 5A). By contrast, siRNA-i was inactive and did not significantly alter the level of the endogenous and transfected proteins. We then tested the effect of the two silencers in the rat β-cell line INS-1E. Under our experimental conditions the transfection efficiency of INS-1E cells was between 30% and 50%. Despite this relatively low transfection rate, a significant decrease in endogenous tomosyn-1 was observed in cells transfected with siRNA-a (Fig. 5B). By contrast, as expected from the data obtained with COS cells, siRNA-i was inactive. As expected,

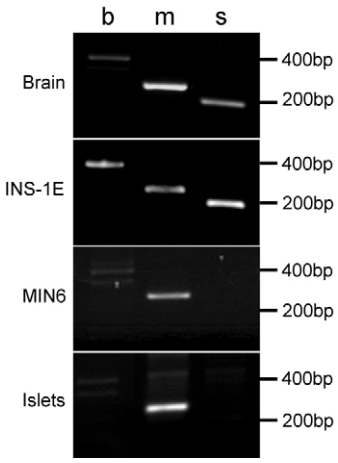

Fig. 2. Determination of the tomosyn-1 isoforms expressed in insulin-secreting cells. The three tomosyn-1 isoforms were amplified by RT-PCR from RNA extracts of rat brain, INS-1E and MIN6 cells and freshly isolated rat pancreatic islets using specific primers. b, b-tomosyn-1; m, m-tomosyn-1; s, s-tomosyn-1

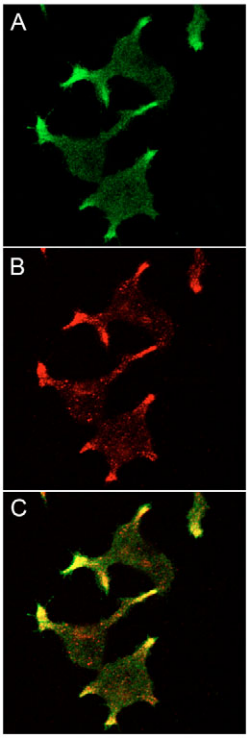

Fig. 3. Subcellular localization of tomosyn-1 in insulin-secreting cells. INS-1E cells were grown on glass coverslips coated with laminin and poly-L-lysine. Then, the cells were fixed with paraformaldehyde and incubated with a rabbit antibody against tomosyn and a guinea pig antibody against insulin. (A) The distribution of tomosyn was analysed by confocal microscopy after labeling with an anti-rabbit antibody coupled to FITC. (B) Secretory granules were visualized with an anti-guinea pig antibody coupled to Cy3. (C) Overlay of images A and B.

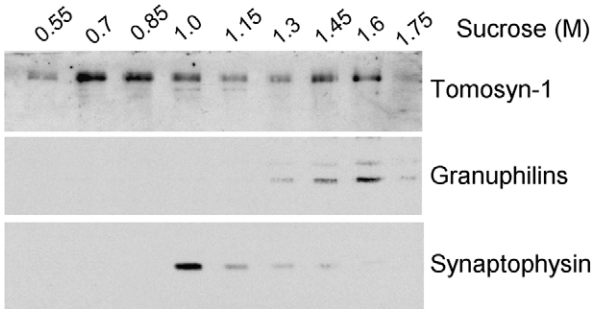

Fig. 4. Analysis of the subcellular distribution of tomosyn-1 on a sucrose density gradient. A post-nuclear supernatant of INS-1E cells was loaded on a sucrose density gradient (0.45-2.0 M) and centrifuged for 18 hours at 110,000 ***g***. Aliquots of the fractions containing 0.55-1.74 M sucrose were analyzed by western blotting using antibodies against tomosyn-1, granuphilin (secretory granule marker) and synaptophysin (synaptic-like vesicle marker).

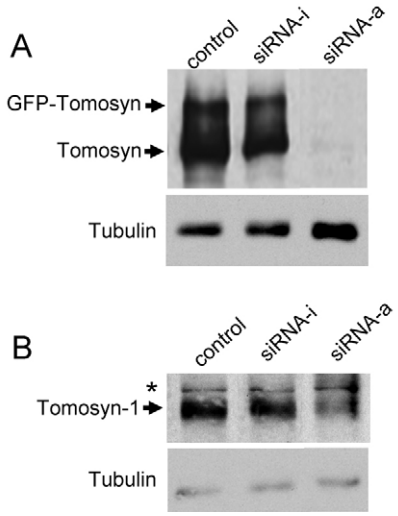

Fig. 5. Effect of short interfering RNAs on tomosyn-1 expression. (A) COS cells were transiently co-transfected with GFP-tagged tomosyn-1 and with empty pSUPER vector (control) or with vectors directing the sequence of two different short interfering RNAs (siRNA-i and siRNA-a). After 3 days the expression level of tomosyn-1 and GFP-tomosyn-1 was analysed by western blotting with a polyclonal antibody against tomosyn-1. The level of tubulin present in the same samples was tested in parallel as a control for protein loading. (B) INS-1E cells were transiently transfected with empty pSUPER vector (control), siRNA-i or siRNA-a. The amount of endogenous tomosyn-1 remaining in the cells after 3 days was assessed by western blotting with antibody against tomosyn-1. Western blotting with antibody against tubulin was performed in parallel as a control for protein loading.

neither siRNA-a nor siRNA-i affected the expression of tubulin.

We then analysed the effect of tomosyn-1 silencing on insulin exocytosis. INS-1E cells were transiently transfected with plasmids leading to the overexpression of rat tomosyn-1 or directing the synthesis of siRNAs. To selectively monitor exocytosis in the fraction of cells that overexpress or lack tomosyn-1, the different constructs were co-transfected with a plasmid encoding the human growth hormone (hGH). Exogenously expressed hGH is targeted to secretory granules of INS-1E cells and is released together with insulin in response to secretagogues (Iezzi et al., 2000). Thus, hGH release allows a direct assessment of exocytosis in cells with altered tomosyn-1 expression. In contrast to previous reports in PC12 and chromaffin cells (Hatsuzawa et al., 2003; Yizhar et al., 2004), overexpression of GFP-tagged rat tomosyn-1 in INS-1E cells did not significantly affect hormone secretion (Fig. 6A). However, the amount of hGH released by the cells transfected with the siRNA capable of reducing tomosyn-1 expression (siRNA-a) was diminished by about 50%. As expected, the secretory response of INS-1E cells transfected with siRNA-i was not altered. To avoid the possibility of off-target effects of siRNA-a, we attempted to rescue the secretory response by replacing endogenous tomosyn-1 with a construct that is not affected by the RNAi process. Mouse tomosyn-1 does not perfectly match the rat nucleotide sequence targeted by siRNA-a and is therefore not affected by the presence of the silencer. As shown in Fig. 6B, introduction of mouse m-tomosyn-1 in cells in which the expression of endogenous tomosyn-1 was blocked by RNAi was sufficient to recover a secretory rate comparable to control cells, confirming the specificity of the effect of siRNA-a (Fig. 6B). As was the case already for GFP-tagged rat tomosyn-1 (Fig. 6A), overexpression of mouse tomosyn-1 did not significantly modify the hormone release (Fig. 6B).

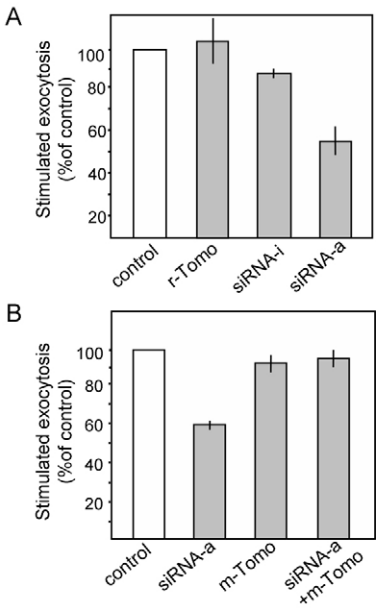

Fig. 6. Effect of up and down regulation of tomosyn-1 expression on exocytosis. (A) INS-1E cells were transiently co-transfected with a plasmid encoding hGH and with the empty pSUPER vector (control), the pEGFP-rat-tomosyn-1, siRNA-i or siRNA-a. After 3 days, the cells were incubated under basal condition or in the presence of stimulatory concentrations of glucose, K^+, forskolin and IBMX. After 45 minutes, the incubation medium was collected. The fraction of hGH released by the cells under basal and stimulatory conditions were measured by ELISA. None of the constructs used in this study affected basal secretion (data not shown). Stimulated exocytosis was defined as the ratio of basal hGH release to the amount of hGh secreted in the presence of glucose, K^+, forskolin and IBMX. The results are the mean of at least three independent experiments measured in triplicates. (B) INS-1E cells were transiently co-transfected with the pSUPER-GH plasmid, encoding both hGH and either the empty pSUPER vector (control) or the siRNA-a, and with either pEGFP or pcDNA3-mouse-tomosyn-1. As described above, cells were incubated under basal condition or in the presence of stimulatory concentrations of glucose, K^+, forskolin and IBMX for 45 minutes. The incubation medium was then collected and the fraction of hGH released by the cells was measured by ELISA. The results are the mean of at least three independent experiments measured in triplicates.

Tomosyn-silencing affects exocytosis at a step beyond Ca^{2+} influx

Next, we attempted to identify the event(s) in the secretory process that are altered in cells lacking tomosyn-1. To obtain more information about the dynamic of the exocytotic process the cells were submitted to repetitive depolarizations (10×300 millisecond-long pulses from –70 mV to 0 mV) and vesicle fusion was assessed by membrane capacitance. In cells transfected with siRNA-i, the total capacitance increase after ten depolarization pulses was 335.2±68.8 fF (n=6) (Fig. 7). In agreement with the secretion experiments presented above, these data were not significantly different from those of cells transfected with an empty pSUPER vector (396.1±50.0 fF, n=8). Silencing of tomosyn-1 with siRNA-a resulted in a capacitance increase that was significantly lower (131.6±21.0 fF, n=9) (Fig. 7). Analysis of the capacitance traces reveals that cells transfected with siRNA-a exhibit an even reduction in membrane capacitance throughout the depolarization train. Indeed, both the total amplitudes of the first two pulses that are likely to reflect fusion from the readily releasable pool of granules and of pulses 3-10, representing fusion of newly recruited granules (Kanno et al., 2004), was reduced by about 60% (Fig. 7).

The decrease in stimulus-induced secretion observed after tomosyn-1 silencing is due to a defect that is distal to glucose-induced Ca^{2+} entry through L-type voltage-gated channels. In fact, tomosyn-1 silencing did not modify the charge/voltage (Q/V) relationship, indicating that ion currents across the plasma membrane are not altered (Fig. 8A). Moreover, the increase in membrane capacitance elicited by direct Ca^{2+} infusion through the patch pipette (Fig. 8B) was also inhibited in cells transfected with siRNA-a (2.95±0.30 fF/s, n=7) compared to controls (4.72±0.52 fF/s, n=8), further demonstrating that tomosyn-1 controls a step beyond Ca^{2+} entry.

Tomosyn-1 is involved in a post-docking event

To assess whether the reduction in vesicle fusion was due to a defect in vesicle docking, the cells were transiently co-transfected with siRNA-a and a plasmid encoding Emerald-IAPP, a fluorescently labeled construct that is targeted to

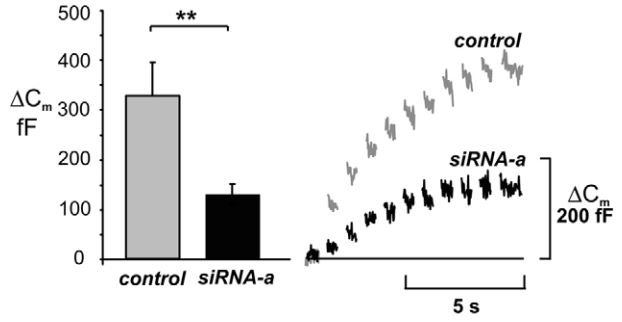

Fig. 7. Capacitance increase after reduction of tomosyn-1 expression. INS-1E cells were transiently transfected with a pSUPER-derived plasmid encoding both GFP and the control siRNA-i (gray) or siRNA-a (black). The transfected cells were identified by EGFP fluorescence and exocytosis was measured by capacitance recordings using the whole-cell configuration of the patch-clamp technique. Exocytosis was triggered by 10×300 ms voltage-clamp depolarizations from –70 mV to 0 mV. $^{**}P<0.01$, significantly different (unpaired *t*-test).

insulin-containing secretory granules (Barg et al., 2002). The number of secretory granules morphologically docked at the plasma membrane was determined by analyzing the cells by total internal reflection fluorescence microscopy (TIRFM). Indeed, using our TIRFM setting, only secretory granules located at less than 100 nm from the plasma membrane were detected. Under resting conditions, the number of granules docked at the plasma membrane in cells lacking tomosyn-1 was not significantly different from control cells (Fig. 9A,B). When exocytosis was triggered, the total number of docked granules of control cells declined gradually. By contrast, consistent with their diminished secretory capacity, in cells lacking tomosyn-1 the total number of docked granules remained rather constant (Fig. 9C). These findings suggest that, despite their close association with the plasma membrane, the secretory granules of cells in which tomosyn-1 is silenced display a diminished capacity to undergo exocytosis. Taken together, our observations indicate that the absence of tomosyn-1 reduces the efficacy of a post-docking event that is required to render insulin-containing secretory granules competent for fusion.

The SNARE-like domain of tomosyn-1 forms a thermodynamically favorable ternary complex with SNAP25 and syntaxin-1

Tomosyn-1 possesses an R-SNARE-like motif analogous to that of VAMP2. To gain insight in to the possible mechanism of action of tomosyn-1, we measured the interaction forces between the R-SNARE-like motif of tomosyn-1 and the Q-SNAREs syntaxin-1 and SNAP25 using atomic force microscopy (Yersin et al., 2003). We found that the interaction force between tomosyn-1 attached to the tip of the cantilever and syntaxin-1 on the mica was 152±9 pN (Fig. 10). Under the same condition, binding to SNAP25 was significantly weaker (109±7 pN). No specific interactions were measured between tomosyn-1 and GST (Fig. 10). As expected, the interaction forces of the SNARE-like motif of tomosyn-1 with a pre-assembled syntaxin-1–SNAP25 complex were higher than those measured with syntaxin-1 or SNAP25 alone (237±13 pN)

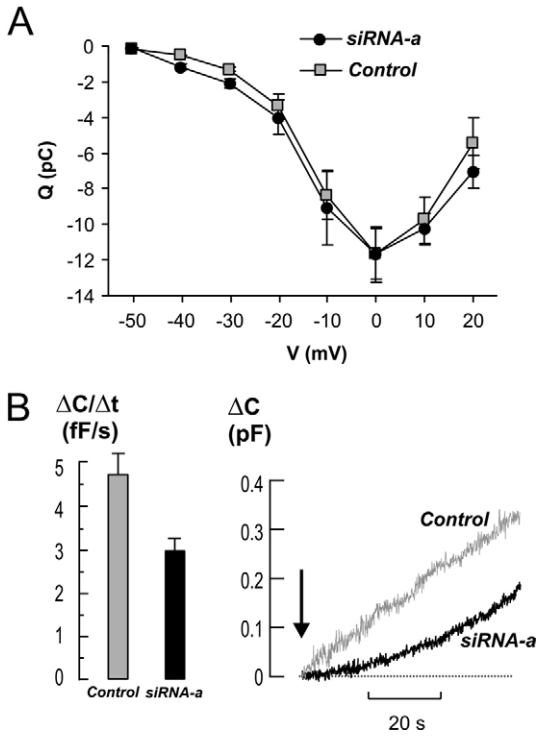

Fig. 8. Tomosyn-1-silencing affects exocytosis at a step beyond Ca^{2+} influx. (A) Charge/voltage (Q/V) relation recorded in siRNA-i-treated cells (control, gray squares) and siRNA-a treated cells (tomosyn-1-silenced, black circles). (B) Ca^{2+} evoked exocytosis. Left: Mean capacitance increase (ΔC/Δt) in control (siRNA-i treated cells, gray bar) and tomosyn-1-silenced cells (siRNA-a, black bar). Exocytosis was elicited by intracellular dialysis of a patch pipette solution containing Ca^{2+}-EGTA buffer (free $[Ca^{2+}]_i$ ~1.5 μM). Right: Examples of capacitance traces from one control and one tomosyn-1-silenced cell (siRNA-a) as indicated. The standard whole-cell configuration was established at *t*=0, indicated by the arrow. $^{*}P<0.05$, significantly different (unpaired *t*-test).

and were comparable to the interaction forces that are observed between VAMP2 and a preassembled syntaxin-1–SNAP25 complex (279±3 pN) (Yersin et al., 2003). Binding to syntaxin-1 and to syntaxin-1–SNAP25 complex was abolished by mutating the residue corresponding to Arg1076 to alanine in the SNARE-like domain of tomosyn-1 (data not shown). Taken together these data indicate that tomosyn-1 can engage in a thermodynamically favorable SNARE-like complex analogous to that formed by VAMP2.

Discussion

The release of hormones and neurotransmitters occurs via a highly coordinated multistep process that involves transport of secretory vesicles to the cell periphery and docking at specific domains of the plasma membrane. Once associated with the cell membrane the docked vesicles undergo a priming step that prepares them for subsequent fusion with the plasma membrane. Some of the key components of the molecular machine controlling exocytosis in pancreatic β-cells have now been identified and include the SNAREs VAMP2, SNAP25 and syntaxin-1. Numerous observations indicate that the assembly of a tripartite complex between these proteins is necessary to

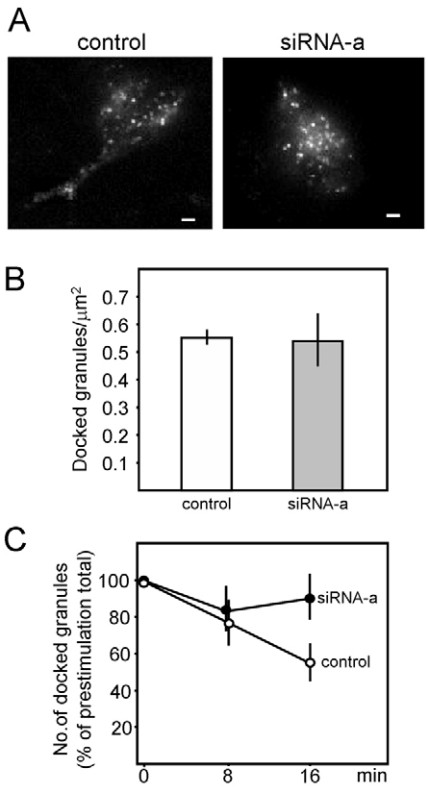

Fig. 9. Effect of tomosyn-1 silencing on the pool of secretory granules docked at the plasma membrane. INS-1E cells were grown on glass coverslips coated with laminin and poly-L-Lysine, and were transiently co-transfected with a plasmid encoding IAPP-Emerald and the pSUPER vector siRNA-i (control) or siRNA-a. Three days later the transfected cells were visualized by TIRF microscopy (A). Single IAPP-Emerald-EGFP-positive granules from nine control cells and nine cells transfected with siRNA-a were manually selected and counted. The number of IAPP-Emerald-EGFP-positive granules was then divided by the single cell area. (B) Results of the experiments in from A, expressed as means ± s.e.m. (C) Six control cells and six cells transfected with siRNA-a were incubated in the presence of stimulatory concentrations of glucose, K^+, forskolin and IBMX. Single IAPP-Emerald-EGFP-positive granules were manually selected and counted after 0, 8 and 16 minutes of incubation in the presence of the stimuli. Data are expressed as means ± s.e.m. *P<0.01, significantly different (unpaired t-test).

drive the fusion of insulin-containing granules with the plasma membrane (for reviews, see Lang, 1999; Easom, 2000; Rorsman and Renström, 2003).

In this study we have investigated the involvement in the regulation of insulin secretion of tomosyn-1, a syntaxin-1-binding protein with SNARE-like properties. We found that pancreatic β-cells possess different isoforms of tomosyn-1, including the brain-specific m- and s-isoforms, further confirming that pancreatic β-cells and neurons share many of the components of the molecular machinery that control exocytosis (Lang, 1999). The three tomosyn-1 isoforms do not possess hydrophobic domains susceptible to directly anchor them to cellular membranes. However, in line with a possible involvement in the regulation of insulin release, tomosyn-1 was not homogenously distributed in the cytoplasm but rather localized together with secretory granules at the cell periphery.

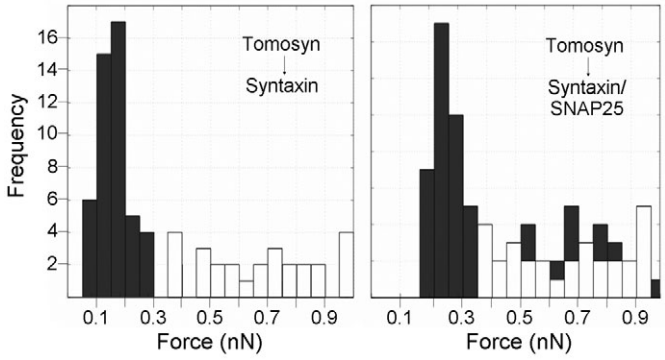

Fig. 10. Measurement of the interaction forces between the R-SNARE-like motif of tomosyn-1 and the Q-SNAREs syntaxin-1 and SNAP-25. A GST-fusion protein containing the SNARE-like motif of tomosyn-1 was fixed to the cantilever of the AFM. Syntaxin-1 (left panel) or the syntaxin-1-SNAP25 complex (right panel) were attached on the mica. The histograms show the frequencies of the forces of the specific events (gray bars). White bars indicate the frequencies and forces of nonspecific events measured using GST-covered mica. The mean unbinding forces were 152±9 and 237±13 pN for the interactions with syntaxin-1 and with the syntaxin-1-SNAP25 complex, respectively.

Enrichment of the protein in specific cellular compartments is probably governed by interaction with other cellular components possibly mediated by the numerous WD repeats contained in the tomosyn-1 sequence. Tomosyn-1 is part of a family that includes the yeast proteins Sro7 and Sro77 and the *Drosophila* tumor supressor *lethal giant larvae* (Lgl). Yeast and *Drosophila* family members have been shown to bind to unconventional myosins (Strand et al., 1994; Gangar et al., 2005). Future experiments will have to assess whether the localization of tomosyn-1 is dictated by interaction with cytoskeletal elements surrounding the secretory granules.

Tomosyn-1 has been suggested to exert an inhibitory control on exocytosis in PC12 and chromaffin cells, and in neurons. In these cells, overexpression of tomosyn-1 leads to a reduction in catecholamine release (Fujita et al., 1998; Hatsuzawa et al., 2003; Yizhar et al., 2004; Baba et al., 2005). This effect was assumed to be due to the formation of non-functional SNARE complexes with syntaxin-1. However, recently tomosyn-1 mutants defective in syntaxin-1-binding were found to inhibit exocytosis to a greater extent than the wild-type protein implying a different mode of action (Constable et al., 2005). In this study, overexpression of tomosyn-1 in β-cells did not significantly affect secretion. There are several plausible explanations for this finding. First, under our experimental conditions the overexpression might not be high enough to inhibit secretion. Considering that in INS-1E cells overexpression is estimated to be close to tenfold (our unpublished data), this possibility appears rather unlikely. Second, the undefined binding partner responsible for the inhibitory effect of tomosyn-1 in catecholamine-secreting cells (Constable et al., 2005) might not be expressed in pancreatic β-cells. In chromaffin cells inhibition of vesicle priming by tomosyn-1 is partially relieved at elevated Ca^{2+} concentrations (Yizhar et al., 2004). Thus, another possible explanation for our findings may reside in differences in the Ca^{2+} sensitivity of the priming apparatus between β-cells and chromaffin cells.

Although overexpression of tomosyn-1 was without consequences on insulin secretion, silencing of the gene by RNAi led to a clear impairment in β-cell exocytosis. Despite almost complete silencing of tomosyn-1, inhibition of exocytosis was only partial. This could signify that there is not an absolute requirement for tomosyn-1 in the priming reaction. Alternatively, tomosyn-2 isoforms might be capable of replacing tomosyn-1. However, so far, attempts to amplify tomosyn-2 isoforms from insulin-secreting cell lines were unsuccessful (our unpublished data). Our finding of a decrease in stimulus-induced exocytosis in β-cells lacking tomosyn-1 is in line with data obtained in yeast for other members of the Lgl family. In fact, in yeast deletion of the two tomosyn homologues Sro7 and Sro77 leads to a severe defect in exocytosis (Lehman et al., 1999). Our results are also consistent with the reduction in neurotransmitter release observed in cultured cervical ganglion neurons after silencing of tomosyn-1 by RNAi (Baba et al., 2005). The absence of tomosyn-1 does not affect early steps in the secretory pathway required for the transport and docking of insulin-containing vesicles. In fact, depolarization-induced Ca^{2+} entry through voltage-gated channels is unaltered and the number of secretory granules in close apposition with the plasma membrane is not significantly different from control cells. However, in the absence of tomosyn-1 the docked granules appear to fuse at a reduced rate with the plasma membrane, suggesting a defect in the priming reaction. Interestingly, overexpression of tomosyn-1 in chromaffin cells results in a similar defect in the secretory process (Yizhar et al., 2004). Thus, the priming machinery might be equally affected by the lack of tomosyn-1 and by the presence of excessive amounts of the protein.

The precise mechanisms by which tomosyn-1 modulates the final steps of the secretory process remain unclear and will need further investigations. Here, we show that in β-cells, tomosyn-1 is localized in close apposition to secretory granules, possibly through the interaction with cytoskeletal elements. We also observed that the protein can form a SNARE-like complex with syntaxin-1 and SNAP25. The interaction forces between the components of this complex are high (237±13 pN) but still significantly lower than those of the complex VAMP2–syntaxin-1–SNAP25 (279±3 pN) (Yersin et al., 2003). We propose that, when the secretory granules approach the plasma membrane tomosyn-1 becomes engaged in a complex with syntaxin-1 and SNAP25. The tomosyn-1–syntaxin-1–SNAP25 complex does not bind complexin and is most probably unable to promote vesicle fusion (Pobbati et al., 2004). Thus, the formation of the tomosyn-1 complex is likely to constitute a transient but necessary event for the final assembly of the VAMP2–syntaxin-1–SNAP25 complex that triggers membrane fusion. Very recently, PKA-mediated phosphorylation of tomosyn-1 on Ser724 was demonstrated to weaken the interaction with syntaxin-1 and to increase the fusion-competent and readily releasable pool of synaptic vesicles (Baba et al., 2005). Activation of the cAMP signaling pathway is known to potentiate exocytosis of pancreatic β-cells (Seino and Shibasaki, 2005). In view of these findings it is tempting to speculate that PKA-mediated phosphorylation of tomosyn-1 is part of the events leading to potentiation of insulin secretion in response to cAMP-raising agents.

In conclusion, we have uncovered an important role for tomosyn-1 in the final steps of the secretory process of pancreatic β-cells. Our data are consistent with an involvement of tomosyn-1 in the cascade of events necessary to prepare insulin-containing secretory granules for fusion. Future studies will have to assess the precise contribution of tomosyn-1 in the determination of the size of the fusion-competent readily releasable granule pool of pancreatic β-cells and will need to pinpoint the role played in this process by PKA-mediated phosphorylation.

Materials and Methods

Material

The pEGFP-tomosyn-1 plasmid and the antibody against tomosyn-1, were generously provided by Reinhard Jahn (University of Göttingen, Germany) (Hatsuzawa et al., 2003). Mouse tomosyn-1 was obtained from Matthijs Verhage (Vrije University Amsterdam, Netherlands). The antibody against insulin was purchased from Linco Research (St Charles, MO). Fluorescently labelled secondary antibodies were from Jackson ImmunoResearch Laboratories (West Grove, PA). The pSUPER plasmid (Brummelkamp et al., 2002) was kindly provided by R. Agami, Netherlands Cancer Institute, Amsterdam.

Immunohistochemistry

Immunohistochemistry was performed on a 2-week-old mouse. The pancreas was isolated after fixation by perfusion with 4% paraformaldehyde in PBS. Twenty-micrometer thick cryosections were incubated overnight at 4°C with primary antibodies. Immunolabeled proteins were visualized by incubating the slices for 1h at room temperature with fluorescently labeled secondary antibodies. Images were obtained by confocal microscopy (Leica, model TCS NT; Lasertechnik, Heidelberg, Germany).

RT-PCR analysis

Total RNA from insulin-secreting INS-1E cells was extracted and reverse transcribed using the retroscript kit (Ambion, Austin, TX). PCR was performed using the Expand high fidelity PCR kit (Roche, Rotkreuz, Switzerland) with primers specific for each isoform. For b-, m- and s-tomosyn-1, we used the following sense primers, respectively: 5′-TCCGACTTCCGGTTCTTCCTC-3′, 5′-TCCGACTTCCGCAAAGATGTC-3′, 5′-TCCGACTTCCGATGTGAAAG-3′. The antisense primer 5′-TTCAGCGTGATGACAAAGGC-3′ was the same for all the reactions.

Cell culture and transfection

The insulin-secreting cell line INS-1E was cultured as previously described (Asfari et al., 1992) in RPMI 1640 supplemented with 5% fetal calf serum (FCS), 50 UI/ml penicillin, 50 μg/ml streptomycin, 0.1 mM sodium pyruvate and 0.001% β-mercaptoethanol. Transient transfection experiments were performed using the Effectene transfection Kit (Qiagen,Valencia, CA) with a DNA:Effectene ratio of 1:25.

Immunocytochemistry

INS-1E was seeded on glass coverslips coated with 20 μg/ml laminin and 2 mg/ml poly-L-lysine. Then, the cells were fixed in 4% paraformaldehyde and incubated for two hours with the first antibody diluted in PBS pH 7.5, 0.1% goat serum, 0.3% Triton X-100 and 20 mg/ml bovine serum albumin (BSA). The coverslips were rinsed with PBS, incubated for 30 minutes with the secondary antibody diluted in the same buffer and mounted for confocal microscopy (Leica, model TCS NT, Lasertechnik, Heidelberg, Germany).

Subcellular fractionation

INS-1E cells were disrupted in 5 mM HEPES (pH 7.4), 1 mM EGTA, 10 μg/ml leupeptin, 2 mg/ml aprotinin and 0.25 M sucrose. The homogenate was then centrifuged for 10 minutes at 3000 ***g*** to eliminate cell debris and nuclei and the supernatant loaded onto a sucrose density gradient (0.4-2.0 M). After 18 hours of centrifugation at 110,000 ***g*** twelve fractions were collected from the top of the gradient and analyzed by western blotting.

Preparation of vectors for tomosyn-1 silencing

Two mammalian expression vectors (siRNA-i and siRNA-a) directing the synthesis of small interfering RNAs targeted against tomosyn-1 were prepared according to the method of Brummelkamp and collaborators (Brummelkamp et al., 2002). Complementary DNA fragments encoding 19-nucleotide sequences derived from rat tomosyn-1 and separated from its reverse 19-nucleotide complement by a short spacer were synthesized by MWG Biotech Company (Germany). For the siRNA-i construct we used the following oligonucleotides: sense, 5′-GATCCCCTGT-GGAGTCCTTCACACTCTTCAAGAGAGAGTGTGAAGGACTCCACATTTTT-GGAAA-3′; antisense, 5′-AGCTTTTCCAAAAATGTGGAGTCCTTCACACTC-TCTCTTGAAGAGTGTGAAGGACTCCACAGGG-3′. For siRNA-a: sense, 5′-

GATCCCCTCTCTTGATAGAGAAGAACTTCAAGAGAGTTCTTCTCTATCAA-GAGATTTTTGGAAA-3′; antisense, 5′-AGCTTTTCCAAAAATCTCTT-GATAGAGAAGAACTCTCTTGAAGTTCTTCTCTATCAAGAGAGGG-3′. The complementary DNA fragments were annealed and cloned in front of the H1-RNA promoter in the pSUPER vector (Brummelkamp et al., 2002). The specificity of each sequence was verified by blast search against the gene data Bank.

Secretion experiments

INS-1E cells were transiently co-transfected with a plasmid encoding hGH and with plasmids encoding either the silencers or the tomosyn expression constructs. Three days later, the cells were pre-incubated for 30 minutes in 20 mM HEPES pH 7.4, 128 mM NaCl, 5 mM KCl, 1 mM $MgCl_2$ and 2.7 mM $CaCl_2$. The medium was then removed and the cells incubated for the indicated periods at 37°C either in the same buffer (basal) or in a buffer containing 20 mM HEPES pH 7.4, 53 mM NaCl, 80 mM KCl, 1 mM $MgCl_2$, 2.7 mM $CaCl_2$, 20 mM glucose, 1 μM Forskolin and 1 mM IBMX (stimulated). Exocytosis from transfected cells was assessed by measuring by ELISA the amount of hGH released in the medium during the incubation period (Roche, Rotkreuz, Switzerland).

Electrophysiology

Exocytosis was measured by capacitance recordings using the whole-cell configuration of the patch-clamp technique. INS-1E cells were cultured in Corning Petri dishes and transfected with pSUPER-GFP siRNA-i or pSUPER-GFP siRNA-a 3 days prior to experiment. During the experiments cells were continuously perfused with pre-heated (34°C) extracellular buffer containing in mM: 118 NaCl, 20 TEA-Cl, 5.6 KCl, 1.2 $MgCl_2$, 2.6 $CaCl_2$, 5 HEPES, 3 glucose, (pH 7.4 with NaOH). Patch electrodes, made from borosilicate glass capillaries, were coated with Sylgard, fire-polished and filled with intracellular pipette solution. For the depolarization-evoked capacitance recordings (Fig. 7) the pipette solution contained: (in mM) 125 Cs-glutamate, 10 NaCl, 10 CsCl, 1 $MgCl_2$, 5 HEPES, 3 Mg-ATP, 0.1 cAMP, 0.05 EGTA; pH 7.2 with CsOH). Exocytosis was here triggered by trains of ten 300 ms voltage-clamp depolarizations from –70 mV to 0 mV. The resulting increase in cell capacitance was recorded using an EPC9 amplifier (HEKA Electronics, Lambrecht/Pfalz, Germany) in conjunction with the HEKA pulse software suite.

For the high-Ca^{2+} infusion experiment (Fig. 8B), the pipette solution contained: (in mM) 125 K-glutamate, 10 KCl, 10 NaCl, 1 $MgCl_2$, 5 HEPES, 3 Mg-ATP, 10 EGTA and 9 $CaCl_2$ (pH 7.2 with KOH). The resulting free intracellular Ca^{2+}-concentration was estimated to 1.5 μM using the binding constant of Martell and Smith. In these experiments exocytosis was measured as the rate of capacitance increase ($\Delta C/\Delta t$) during the first minute after establishment of the whole-cell configuration.

For the charge/voltage (Q/V) relations (Fig. 8A) cells were pre-treated and kept under the same conditions as for the capacitance recordings. Here, Ca^{2+}-currents were elicited by families of 100-millisecond depolarizations from –70 mV to voltages between –50 and +20 mV. The resulting Ca^{2+}-carried charge is plotted against the voltage. In these experiments the pipette solution was the same as for the depolarization-evoked capacitance recordings except for a higher concentration of EGTA (10 mM) to enhance the Ca^{2+}-buffer capacity.

Total internal reflection microscopy imaging

A Zeiss Axiovert 200 inverted fluorescence microscope was modified to allow both EPI and TIRF illumination (Visitron Systems, Puchheim, Germany) as described previously (Bezzi et al., 2004). For TIRF illumination, the expanded beam (488-568 nm argon-krypton multi-line laser, 20 mW; Laserphysics, Stockholm, Sweden) was passed through an AOTF laser wavelength selector (VisiTech international, Sunderland, UK) synchronized with a SNAP-HQ CCD camera (Roper Scientific) under Metafluor software (Universal Imaging) control and introduced from the high numerical aperture objective lens (Zeiss α-plan FLUAR 100X, 1.45 NA). Light entered the coverslip and underwent total internal reflection at the glass-cell interface. Under our experimental conditions, penetration depth of TIRF illumination was approximately 84 nm (Bezzi et al., 2004). For TIRF imaging, INS-1E cells were seeded on glass coverslips coated with 20 μg/ml laminin and 2 mg/ml poly-L-lysine and co-transfected with IAPP-Emerald and empty pSUPER or by IAPP-Emerald and pSUPER-RNAi-a against tomosyn-1. Seventy-two hours later we imaged IAPP-Emerald-EGFP-positive docked granules (Barg et al., 2002) in control cells and cells transfected with siRNA-i and siRNA-a under 488 nm TIRF illumination (Ivarsson et al., 2004). Stimulation was achieved by bath perfusion of 80 mM KCl. Lights were filtered with a beam splitter (Zeiss filter set 10). Video images, digitized with MetaFluor, were analyzed with MetaMorph software (Universal Imaging). To analyze the data, single IAPP-emerald-EGFP-positive granules were manually selected and counted and single cell area was measured. Statistical differences were established using the Student's unpaired *t*-test at $P<0.01$. Data are expressed as mean ± s.e.m.

Atomic force microscopy

The recombinant GST-tagged SNARE proteins syntaxin 1A (lacking the transmembrane region) and SNAP-25 were expressed in DH5-α *E. coli* (Pevsner et al., 1994; Hirling and Scheller, 1996). A GST-fusion protein that included the SNARE-like motif of rat tomosyn-1 (amino acids 1051-1116) was prepared by amplifying the SNARE-like motif from pEFGP-tomosyn-1 with the following primers: sense 5′-GCGGATCCGGGATCGAAGGTGTGAAG-3′; antisense 5′-CGGAGCTCTCAGAACTGGTACCACTTCTT-3′. The amplified cDNA fragment was subcloned in pGEX-KG vector (Guan and Dixon, 1991) in-frame with GST. Arg1076 in the R-SNARE-like motif of rat tomosyn-1 was mutated to alanine by site-directed mutagenesis (Quickchange kit, Stratagene, La Jolla, CA) using the following primers: sense, 5′-CTGGCCCTCGACGAAGCAGGACAGAAG-3′; antisense, 5′-CTTCTGTCCTGCTTCGTCGAGGGCCAG-3′. Mutagenesis was verified by sequence analysis. The bacterial proteins were purified by glutathione-agarose affinity chromatography. Proteins were eluted with 10 mM glutathione in 50 mM Tris-HCl pH 8. The GST tag was not removed in order to decrease the probability of crosslinking in the binding regions of SNAREs. Freshly purified proteins were stored overnight at 4°C before use.

Recombinant proteins (200–300 ng/μl) were crosslinked with glutaraldehyde (0.5%, 15-min incubation) to a freshly cleaved mica sheet functionalized by aminopropyltriethoxysilan (Janowski et al., 1991). This method has been previously demonstrated to preserve protein function (Allen et al., 1997; Allen et al., 1999). The GST-fusion protein containing the SNARE-like motif of tomosyn-1 (200–300 ng/μl) was attached to the AFM tip by 15-min incubation in glutaraldehyde (0.5%). Premixed binary complexes were obtained by mixing two proteins in equal concentrations (overnight at 4°C) before crosslinking to mica with glutaraldehyde. Atomic Force Microscopy (AFM) experiments were performed at room temperature on a Nanoscope III (Digital Instruments, Santa Barbara, CA) using force volume mode operating in liquid. Measurements were done in TBS buffer with a constant retraction speed of 355 nm/s. We used standard triangular Si_3N_4 AFM cantilevers from Veeco (Santa Barbara, CA) with a 0.06 N/m nominal spring constant calibrated as described (Hutter and Bechhoefer, 1993). Force curves were analyzed off-line by a home made fuzzy logic algorithm (Kasas et al., 2000). Each experiment was repeated independently at least five times.

We are indebted to G. Dietler, EPFL, Lausanne, for giving us the opportunity to use the atomic force microscope in his Laboratory and with A. Abderrahmani for providing freshly isolated pancreatic islets. We thank S. Gattesco and F. Dolivo for skilful technical assistance. We are also grateful to R. Jahn, M. Verhage and R. Agami for providing plasmids and antibodies. This work was supported by Swiss National Science Foundation Grant 3200B0-101746.

References

Allen, S., Chen, X., Davies, J., Davies, M. C., Dawkes, A., Edwards, J. C., Roberts, C. J., Sefton, J., Tendler, S. J. B. and Williams, P. M. (1997). Detection of antigen-antibody binding events with the atomic force microscope. *Biochemistry* **36**, 7457-7463.

Allen, S., Davies, J., Davies, M. C., Dawkes, A., Roberts, C. J., Tendler, S. J. B. and Williams, P. M. (1999). The influence of epitope availability on atomic-force microscope studies of antigen-antibody interactions. *Biochem. J.* **341**, 173-178.

Asfari, M., Janjic, D., Meda, P., Li, G., Halban, P. A. and Wollheim, C. B. (1992). Establishment of 2-mercaptoethanol-dependent differentiated insulin-secreting cell lines. *Endocrinology* **130**, 167-178.

Baba, T., Sakisaka, T., Mochida, S. and Takai, Y. (2005). PKA-catalyzed phosphorylation of tomosyn and its implication in Ca^{2+}-dependent exocytosis of neurotransmitter. *J. Cell Biol.* **170**, 1113-1125.

Barg, S., Olofsson, C. S., Schriever-Abeln, J., Wendt, A., Gebre-Medhin, S., Renstrom, E. and Rorsman, P. (2002). Delay between fusion pore opening and peptide release from large dense-core vesicles in neuroendocrine cells. *Neuron* **33**, 287-299.

Bezzi, P., Gundersen, V., Galbete, J. L., Seifert, G., Steinhauser, C., Pilati, E. and Volterra, A. (2004). Astrocytes contain a vesicular compartment that is competent for regulated exocytosis of glutamate. *Nat. Neurosci.* **7**, 613-620.

Bock, J. B., Matern, H. T., Peden, A. A. and Scheller, R. H. (2001). A genomic perspective on membrane compartment organization. *Nature* **409**, 839-841.

Brummelkamp, T. R., Bernards, R. and Agami, R. (2002). A system for stable expression of short interfering RNAs in mammalian cells. *Science* **296**, 550-553.

Cheviet, S., Coppola, T., Haynes, L. P., Burgoyne, R. D. and Regazzi, R. (2004). The Rab-binding protein Noc2 is associated with insulin-containing secretory granules and is essential for pancreatic beta-cell exocytosis. *Mol. Endocrinol.* **18**, 117-126.

Constable, J. R., Graham, M. E., Morgan, A. and Burgoyne, R. D. (2005). Amisyn regulates exocytosis and fusion pore stability by both syntaxin-dependent and syntaxin-independent mechanisms. *J. Biol. Chem.* **280**, 31615-31623.

Easom, R. A. (2000). Beta-granule transport and exocytosis. *Semin. Cell Dev. Biol.* **11**, 253-266.

Fasshauer, D., Sutton, R. B., Brunger, A. T. and Jahn, R. (1998). Conserved structural features of the synaptic fusion complex: SNARE proteins reclassified as Q- and R-SNAREs. *Proc. Natl. Acad. Sci. USA* **95**, 15781-15786.

Fujita, Y., Shirataki, H., Sakisaka, T., Asakura, T., Ohya, T., Kotani, H., Yokoyama, S., Nishioka, H., Matsuura, Y., Mizoguchi, A. et al. (1998). Tomosyn: a syntaxin-1-

binding protein that forms a novel complex in the neurotransmitter release process. *Neuron* **20**, 905-915.

Gangar, A., Rossi, G., Andreeva, A., Hales, R. and Brennwald, P. (2005). Structurally conserved interaction of Lgl family with SNAREs is critical to their cellular function. *Curr. Biol.* **15**, 1136-1142.

Gerst, J. E. (2003). SNARE regulators: matchmakers and matchbreakers. *Biochim. Biophys. Acta* **1641**, 99-110.

Groffen, A. J., Jacobsen, L., Schut, D. and Verhage, M. (2005). Two distinct genes drive expression of seven tomosyn isoforms in the mammalian brain, sharing a conserved structure with a unique variable domain. *J. Neurochem.* **92**, 554-568.

Guan, K. L. and Dixon, J. E. (1991). Eukaryotic proteins expressed in Escherichia coli: an improved thrombin cleavage and purification procedure of fusion proteins with glutathione S-transferase. *Anal. Biochem.* **192**, 262-267.

Hatsuzawa, K., Lang, T., Fasshauer, D., Bruns, D. and Jahn, R. (2003). The R-SNARE motif of tomosyn forms SNARE core complexes with syntaxin 1 and SNAP-25 and down-regulates exocytosis. *J. Biol. Chem.* **278**, 1159-1166.

Hirling, H. and Scheller, R. H. (1996). Phosphorylation of synaptic vesicle proteins: modulation of the alpha SNAP interaction with the core complex. *Proc. Natl. Acad. Sci. USA* **93**, 11945-11949.

Hutter, J. L. and Bechhoefer, J. (1993). Calibration of atomic-force microscope tips. *Rev. Sci. Instrum.* **64**, 1868-1873.

Iezzi, M., Regazzi, R. and Wollheim, C. B. (2000). The Rab3-interacting molecule RIM is expressed in pancreatic beta-cells and is implicated in insulin exocytosis. *FEBS Lett.* **474**, 66-70.

Ivarsson, R., Obermuller, S., Rutter, G. A., Galvanovskis, J. and Renström, E. (2004). Temperature-sensitive random insulin granule diffusion is a prerequisite for recruiting granules for release. *Traffic* **5**, 750-762.

Janowski, F., Fischer, G., Urbaniak, W., Foltynowicz, Z. and Marciniec, B. (1991). Aminopropylsilane treatment for the surface of porous glasses suitable for enzyme immobilisation. *J. Chem. Tech. Biotechnol.* **51**, 263-272.

Kanno, T., Ma, X., Barg, S., Eliasson, L., Galvanovskis, J., Gopel, S., Larsson, M., Renstrom, E. and Rorsman, P. (2004). Large dense-core vesicle exocytosis in pancreatic beta-cells monitored by capacitance measurements. *Methods* **33**, 302-311.

Kasas, S., Riederer, B. M., Catsicas, S., Capella, B. and Dietler, G. (2000). Fuzzy logic algorithm to extract specific interaction forces from atomic force microscopy data. *Rev. Sci. Instrum.* **71**, 2082-2086.

Lang, J. (1999). Molecular mechanisms and regulation of insulin exocytosis as a paradigm of endocrine secretion. *Eur. J. Biochem.* **259**, 3-17.

Lehman, K., Rossi, G., Adamo, J. E. and Brennwald, P. (1999). Yeast homologues of tomosyn and lethal giant larvae function in exocytosis and are associated with the plasma membrane SNARE, Sec9. *J. Cell Biol.* **146**, 125-140.

Masuda, E. S., Huang, B. C., Fisher, J. M., Luo, Y. and Scheller, R. H. (1998). Tomosyn binds t-SNARE proteins via a VAMP-like coiled coil. *Neuron* **21**, 479-480.

Mayer, A. (2001). What drives membrane fusion in eukaryotes? *Trends Biochem. Sci.* **26**, 717-723.

Pevsner, J., Hsu, S. C., Braun, J. E., Calakos, N., Ting, A. E., Bennett, M. K. and Scheller, R. H. (1994). Specificity and regulation of a synaptic vesicle docking complex. *Neuron* **13**, 353-361.

Pobbati, A. V., Razeto, A., Boddener, M., Becker, S. and Fasshauer, D. (2004). Structural basis for the inhibitory role of tomosyn in exocytosis. *J. Biol. Chem.* **279**, 47192-47200.

Rorsman, P. and Renstrom, E. (2003). Insulin granule dynamics in pancreatic beta cells. *Diabetologia* **46**, 1029-1045.

Sakisaka, T., Baba, T., Tanaka, S., Izumi, G., Yasumi, M. and Takai, Y. (2004). Regulation of SNAREs by tomosyn and ROCK: implication in extension and retraction of neurites. *J. Cell Biol.* **166**, 17-25.

Seino, S. and Shibasaki, T. (2005). PKA-dependent and PKA-independent pathways for cAMP-regulated exocytosis. *Physiol. Rev.* **85**, 1303-1342.

Strand, D., Jakobs, R., Merdes, G., Neumann, B., Kalmes, A., Heid, H. W., Husmann, I. and Mechler, B. M. (1994). The Drosophila lethal(2)giant larvae tumor suppressor protein forms homo-oligomers and is associated with nonmuscle myosin II heavy chain. *J. Cell Biol.* **127**, 1361-1373.

Yersin, A., Hirling, H., Steiner, P., Magnin, S., Regazzi, R., Huni, B., Huguenot, P., De los Rios, P., Dietler, G., Catsicas, S. et al. (2003). Interactions between synaptic vesicle fusion proteins explored by atomic force microscopy. *Proc. Natl. Acad. Sci. USA* **100**, 8736-8741.

Yizhar, O., Matti, U., Melamed, R., Hagalili, Y., Bruns, D., Rettig, J. and Ashery, U. (2004). Tomosyn inhibits priming of large dense-core vesicles in a calcium-dependent manner. *Proc. Natl. Acad. Sci. USA* **101**, 2578-2583.

Yokoyama, S., Shirataki, H., Sakisaka, T. and Takai, Y. (1999). Three splicing variants of tomosyn and identification of their syntaxin-binding region. *Biochem. Biophys. Res. Commun.* **256**, 218-222.